
# Functional Source Imaging of Spinal Cord Activity From Its Evoked Magnetic Field

**Kensuke Sekihara**

Department of Systems Design & Engineering
Tokyo Metropolitan University

# Research team

## Clinical evaluation

**Tokyo Medical and Dental University**
**Section of Orthopedic and Spinal Surgery**

- Shigenori Kawabata
- Senichi Ishii
- Shoji Tomizawa
- Masaki Tomori
- Kyohei Sakaki

## Hardware development

**Kanazawa Institute of Technology**
**Applied Electronics Laboratory**

- Yoshiaki Adachi
- Gen Uehara
- Hisanao Ogata
- Hisashi Kado

## Analysis methods

**Tokyo Metropolitan University**

- Tomoya Sato
- Ryohei Nakamura
- Susumu Fuji
- Yoshihide Kawada
- Shuhei Nakamoto
- Taishi Watanabe
- Kosuke Okamoto

## Project coordinator

**Yokogawa Electric Co.**

- Yasuhiro Haruta

# A nerve conduction block of the cervical spinal cord

**This anatomical MRI shows the cervical spinal cord compressed by intervertebral disks and ligaments**

**If a nerve conduction abnormality exists, it may cause numbness and paralysis in the limbs.**

**Such spinal cord conduction disorders are common, and the number of patients exceeds four hundred thousand in Japan.**

**Problem: compression and other spinal cord abnormalities found on patient's anatomical images do not always cause spinal cord disorders.**

Need for functional measurement of spinal cord activity

# Spinal-cord-evoked potential measurements

An existing method for functional measurement of spinal cord activity.

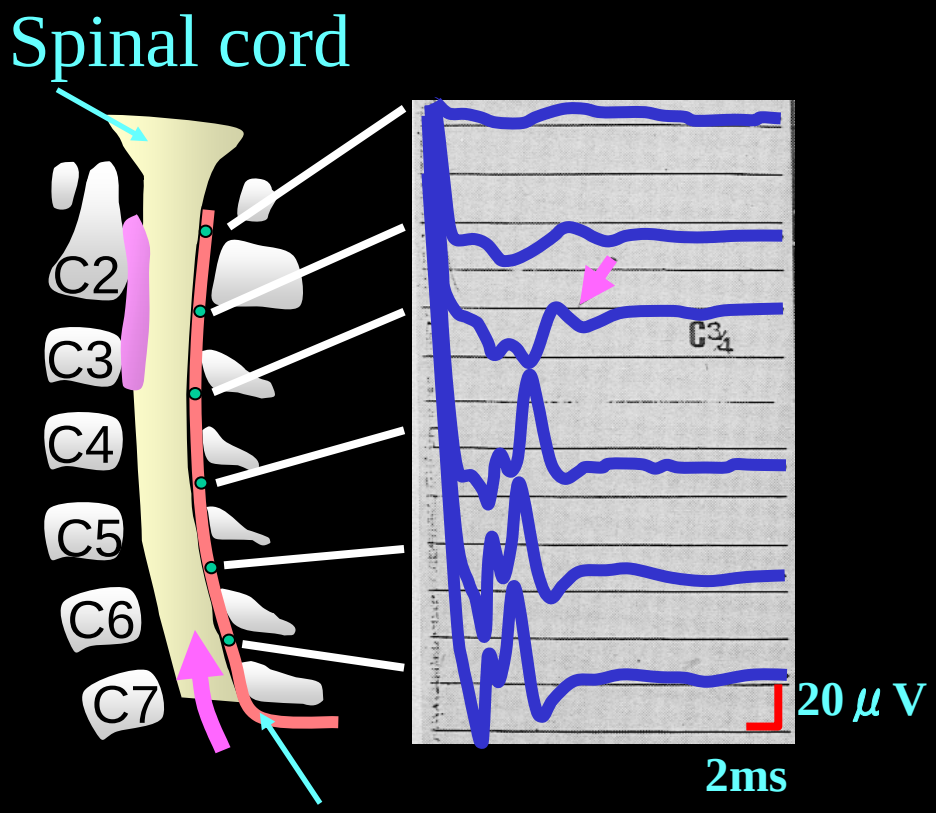


**The SCEP measurement requires inserting an electrode array in the epidural space of a patient.**

**The stimulus is applied at patient's sciatic nerve, and stimulus evoked potential is measured at each electrode.**

**By looking at the reduction of the peak height of the electrode time courses, the location of a nerve conduction block is identified.**

**Problem: Because highly skilled techniques are needed for this electrode insertion, such measurement has been carried out only at a limited number of hospitals.**

# We have developed spinal cord source imaging system using spinal cord evoked magnetic field.

Biomagnetometer for SCEF measurements

Sensor outputs of SCEF

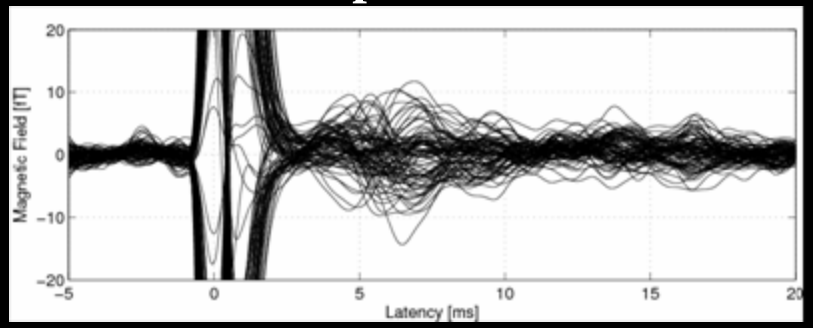


Image of spinal-cord electrical activity

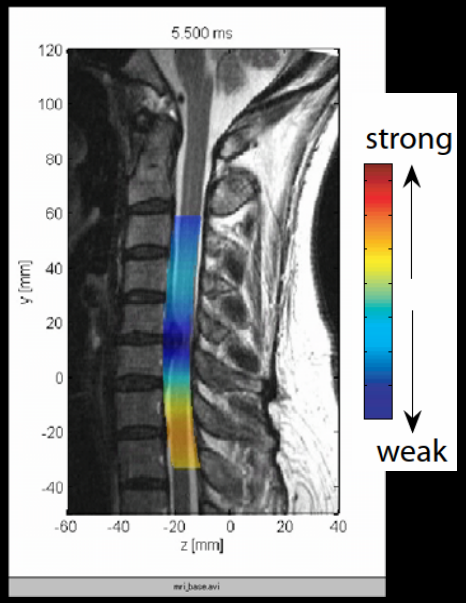


I am going to talk about this imaging system with emphasis on our analysis method to detect spinal cord conduction abnormalities.

# Source model of spinal cord electrical activity

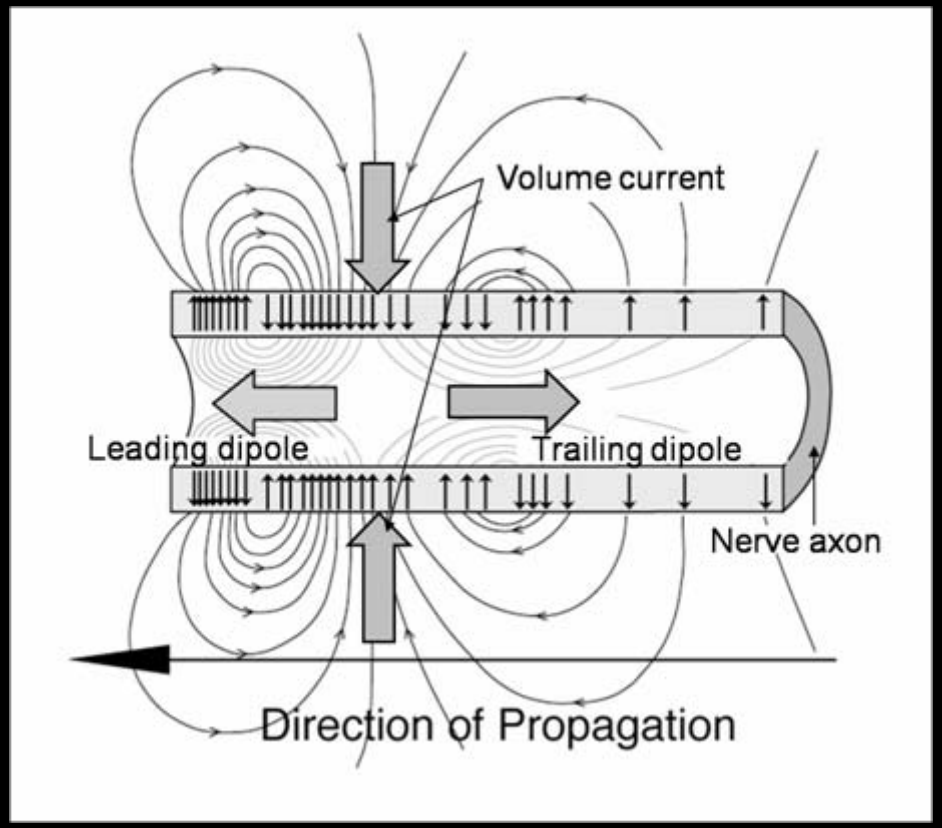


- Within the nerve axon, we have two cellular currents called the leading and the trailing dipoles; they are directed in the opposite directions.

- Our experiments show that we should consider volume currents flowing into the middle between the leading and the trailing dipoles.

- At this location, the volume currents are concentrated and look like dipoler currents

# Spinal-cord evoked magnetic field (SEMF)

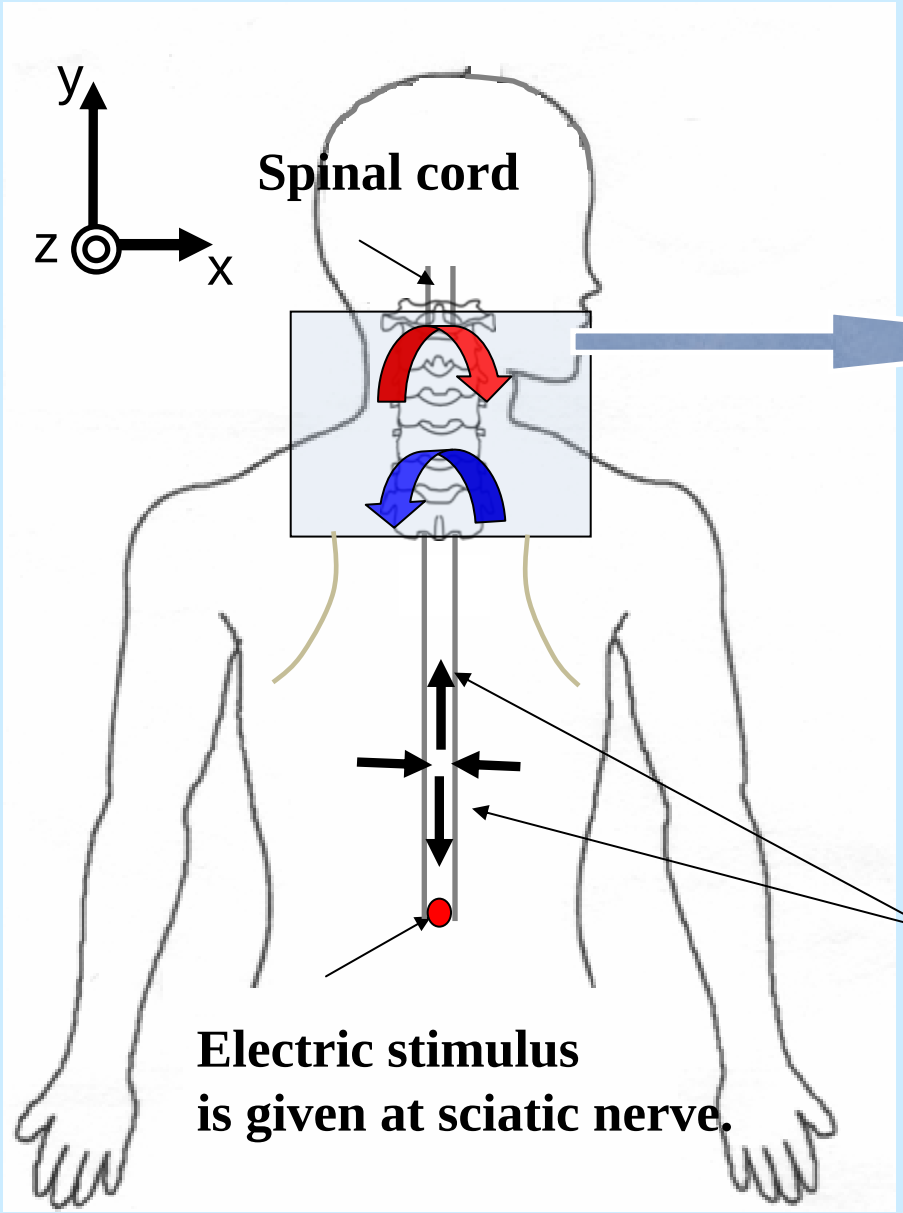


**The magnetic field such as the one below is measured by sensors located near the subject'neck.**

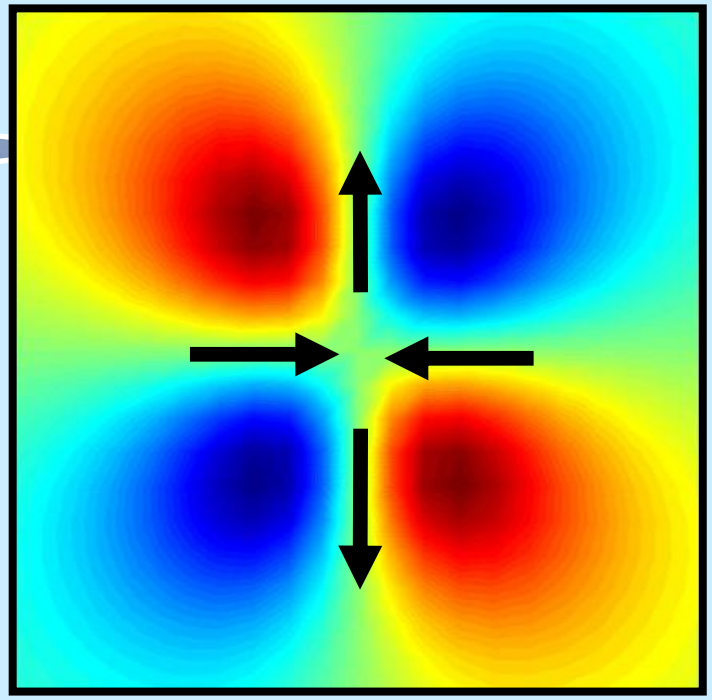

**The stimulus elicites the nerve activity travelling toward the head.**

# Animal Experiments

# Measurement hardware used for animal experiments

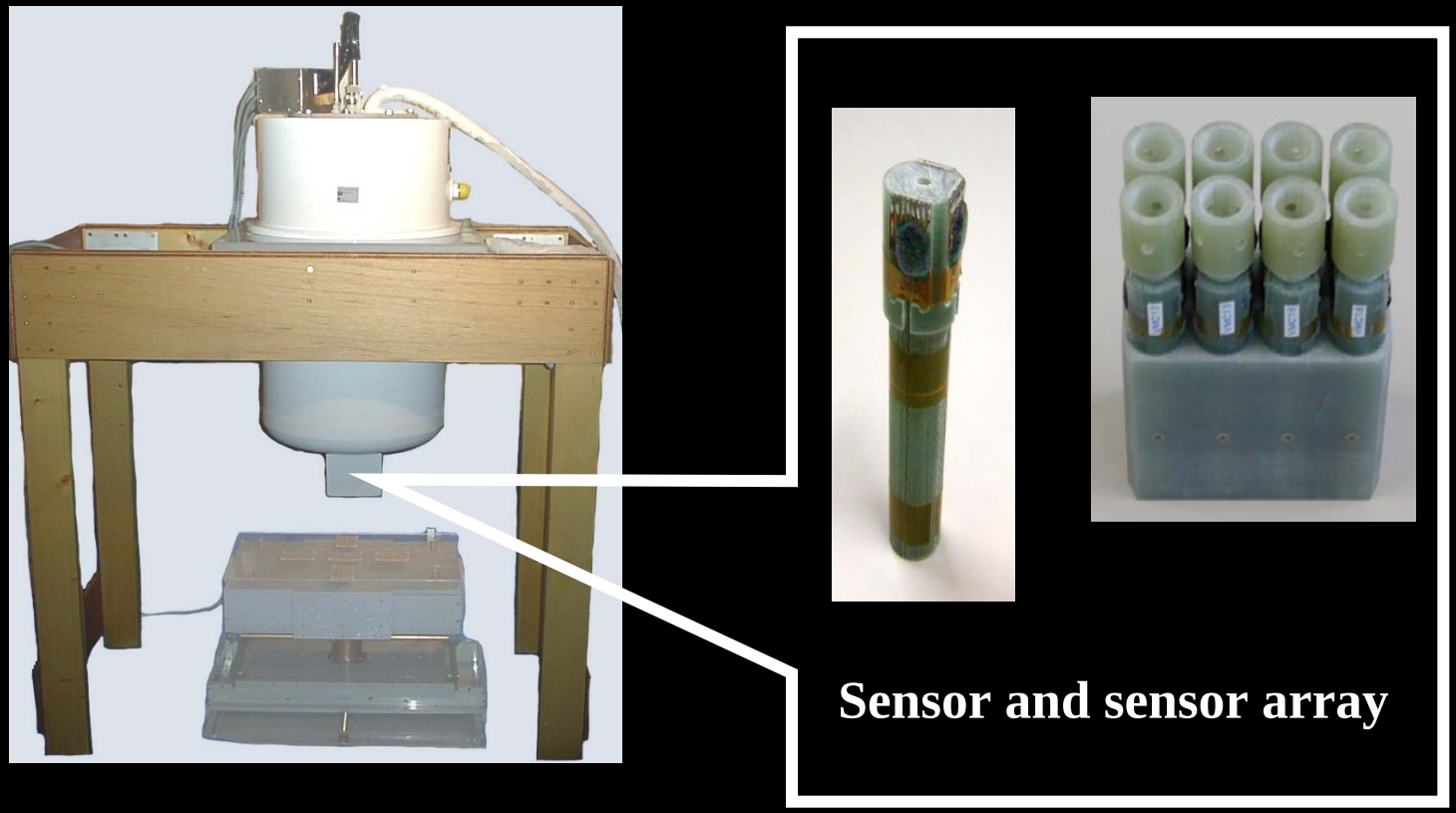


- **This is our the home made biomagnetometer designed for measurements using small animals.**
- **We developed hardware for human measurements, based on this animal model.**

Y. Adachi, *et al., Supercond. Sci. Technol.,* vol. 14, pp. 1075–1080, 2001.

# SCEF was measured from an anesthetized rabbit

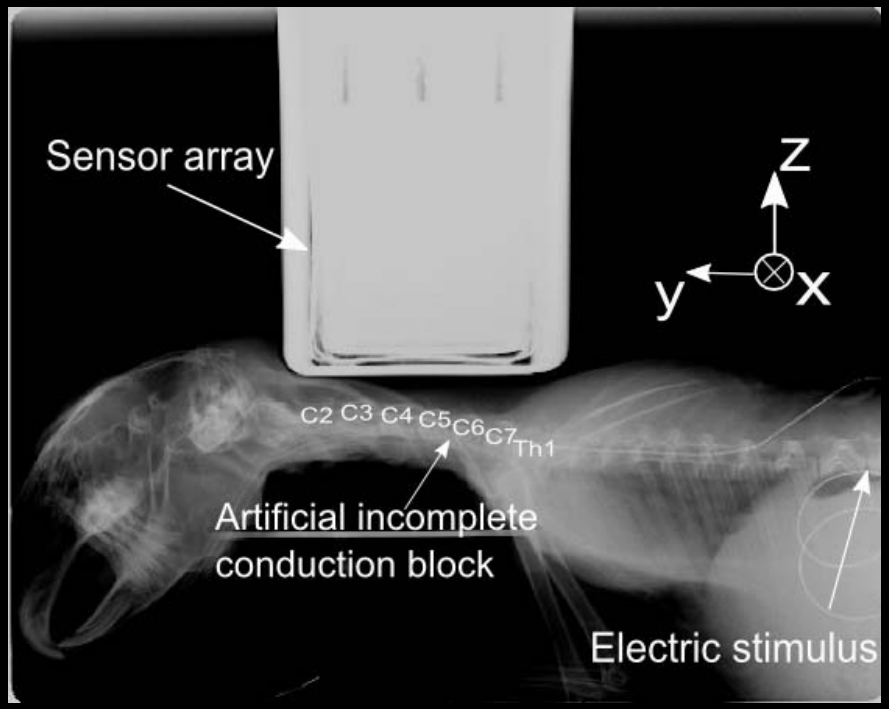


X-ray image showing relative position between rabbit vertebrae and sensors.

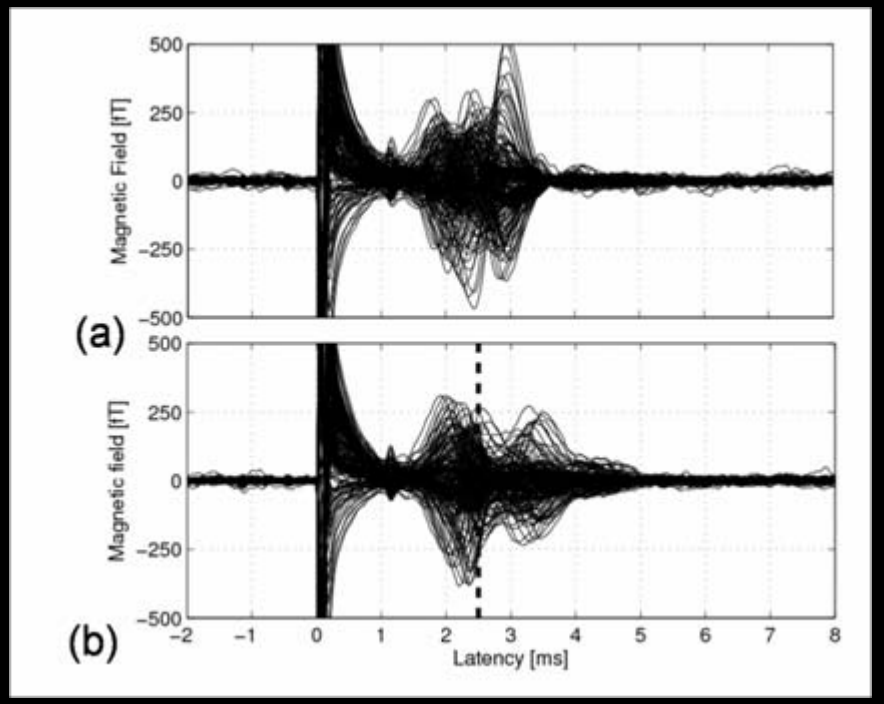


SCEF time courses measured before and after the conduction block was created.

- A catheter with a balloon tip was inserted into the cervical epidural space.
- An artificial incomplete conduction block was created by inflating the balloon between the fifth (C5) and the sixth vertebra (C6).

# Spatial-filter source imaging

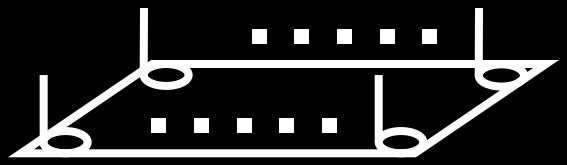

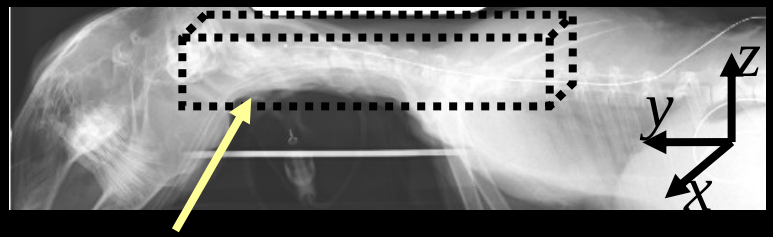


Reconstruction region is set to cover the spinal cord

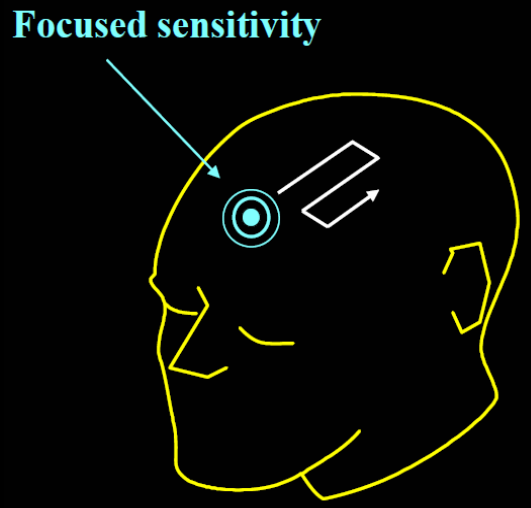


## Mathematical formulation

$$\hat{s}(\boldsymbol{r},t) = \boldsymbol{w}^T(\boldsymbol{r})\boldsymbol{b}(t) = [w_1(\boldsymbol{r}),\ldots,w_M(\boldsymbol{r})]\begin{bmatrix} b_1(t) \\ \vdots \\ b_M(t) \end{bmatrix} = \sum_{m=1}^{M} w_m(r)b_m(t)$$

## sLORETA (Pasucual-Marque)

$$\boldsymbol{w}(\boldsymbol{r}) = \boldsymbol{G}^{-1}\boldsymbol{l}(\boldsymbol{r}) / \sqrt{\boldsymbol{l}^T(\boldsymbol{r})\boldsymbol{G}^{-1}\boldsymbol{l}(\boldsymbol{r})}$$

The spatial filter reconstructs source activity by applying a location dependent weight to the measured data. The filter combines the sensitivity of sensors to create a focused sensitivity region.

# Reconstructed spinal cord activity of anesthetized rabbit

**Artificial conduction block**

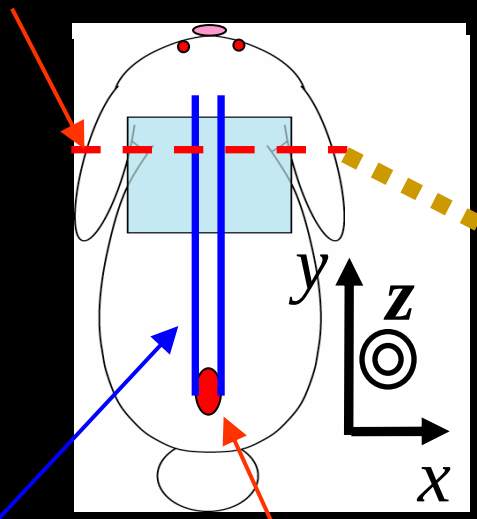


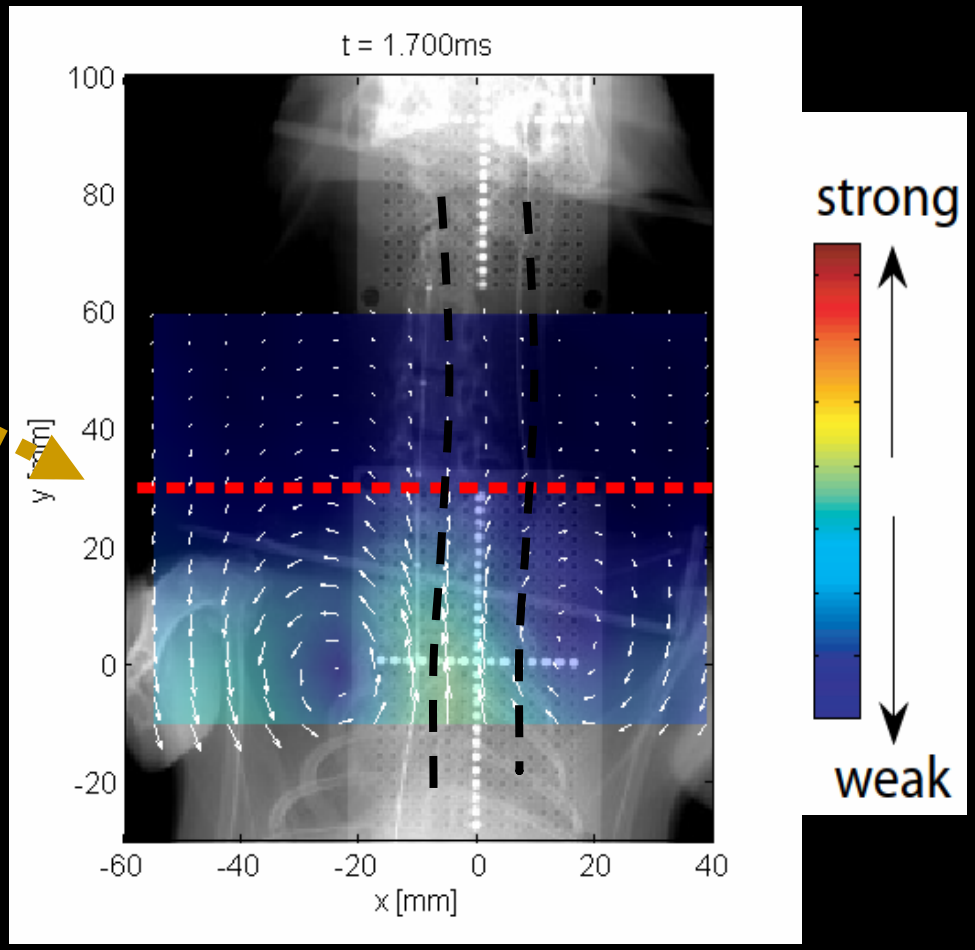


**No conductor model is used to compute the lead field.**

- **The two dipole currents seem to be less affected by the conduction block.**
- **The intensity of the volume currents rapidly decreases around the location of the conduction block.**

# Plot of reconstructed time courses

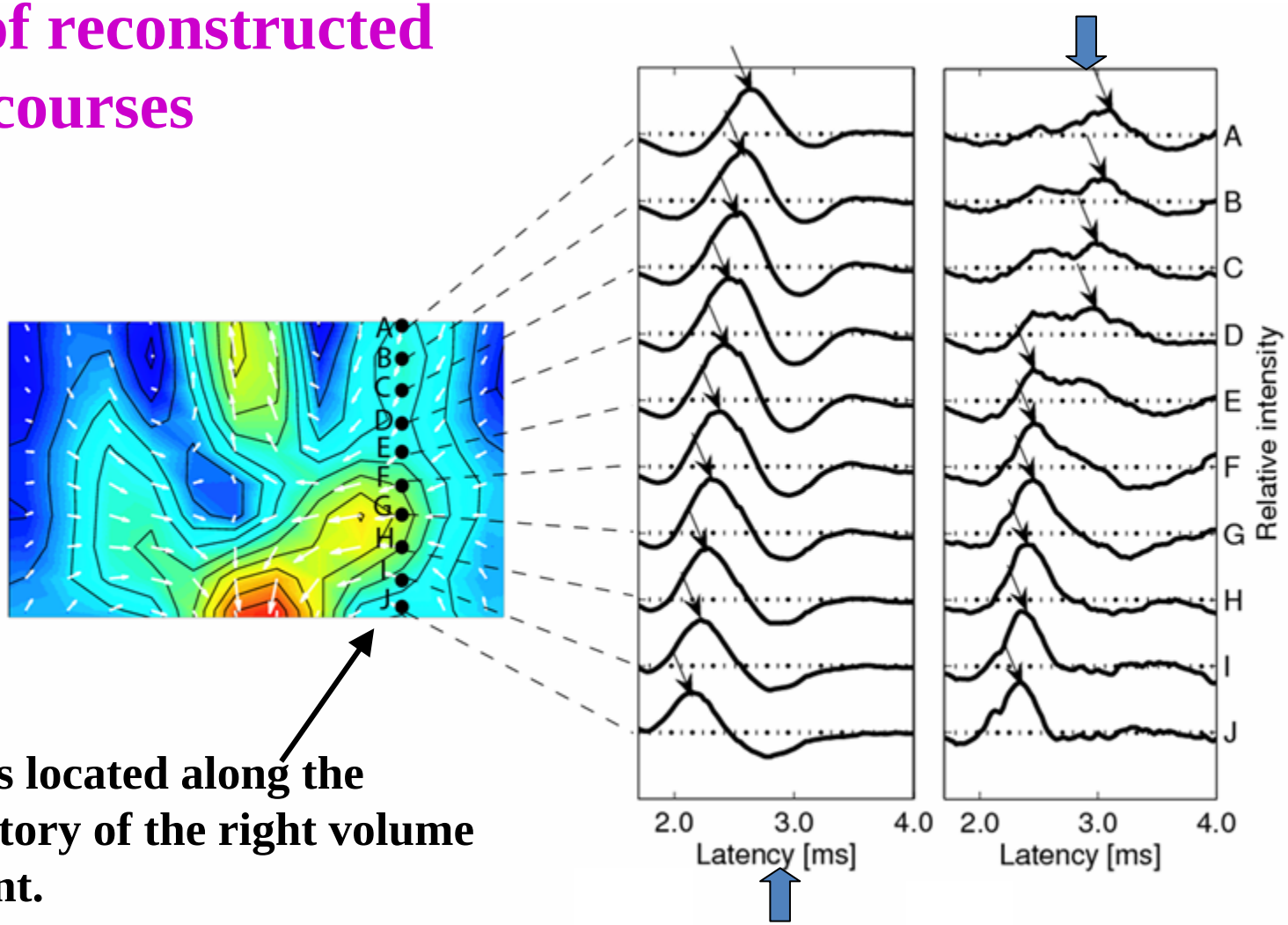


**The artificial conduction block was introduced between the voxels labeled “D” and “E”. The peak intensity significantly changes there.**

# Plots of peak amplitude and latency of the voxel time courses

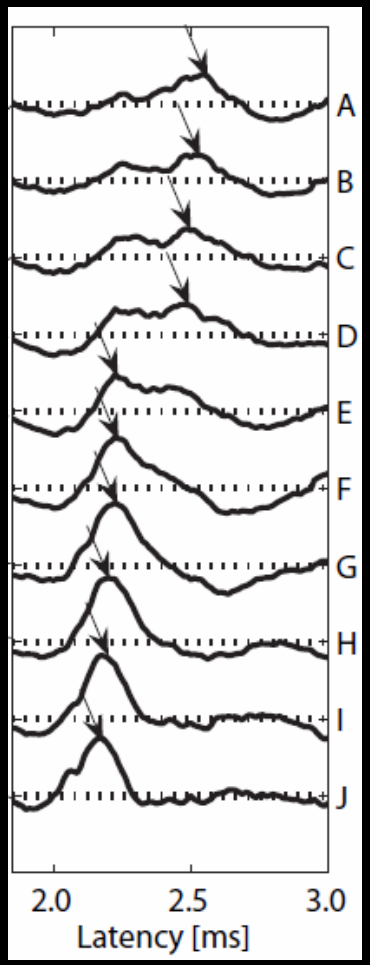


## Location of conduction block

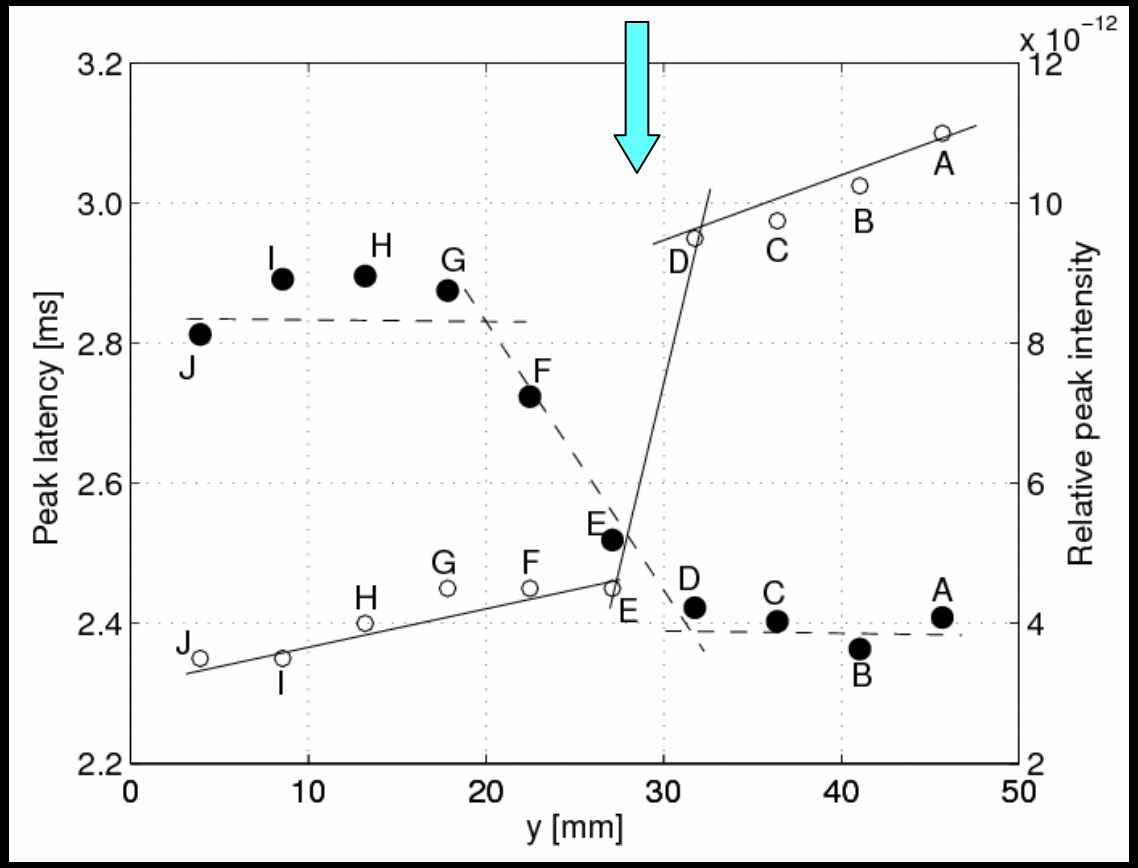


**Significant changes in the latency and intensity of the peaks can be observed near the conduction block, indicating that these quantities can be indicators of the spinal cord conduction abnormality.**

# Human Experiments

•We then conducted imaging experiments using human subjects.

•The main purpose is to check whether we can detect locations of spinal cord conduction abnormalities from the properties of the volume currents.

# Biomagnetometer for human SCEF measurements
# Cryostat and sensors

**The cryostat has a cylindrical body with this protrusion part which contains sensors in the upward direction.**

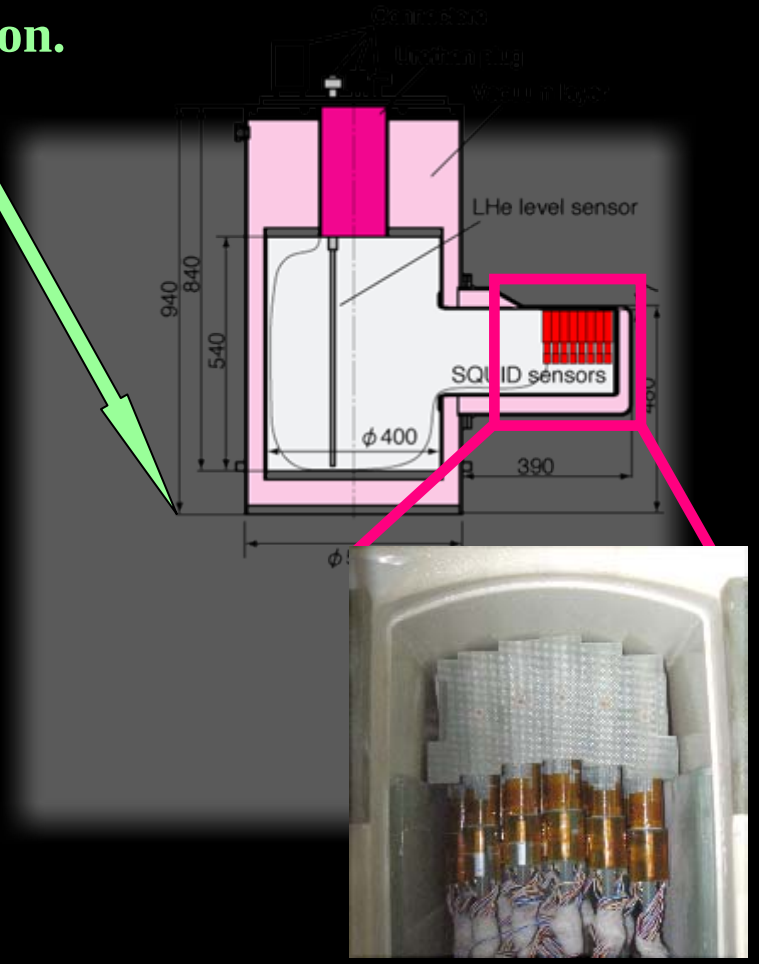




**A subject lies down in the supine position, and the subject's lower neck is positioned on the upper surface of the protrusion of the cryostat.**

# Vector SQUID gradiometer

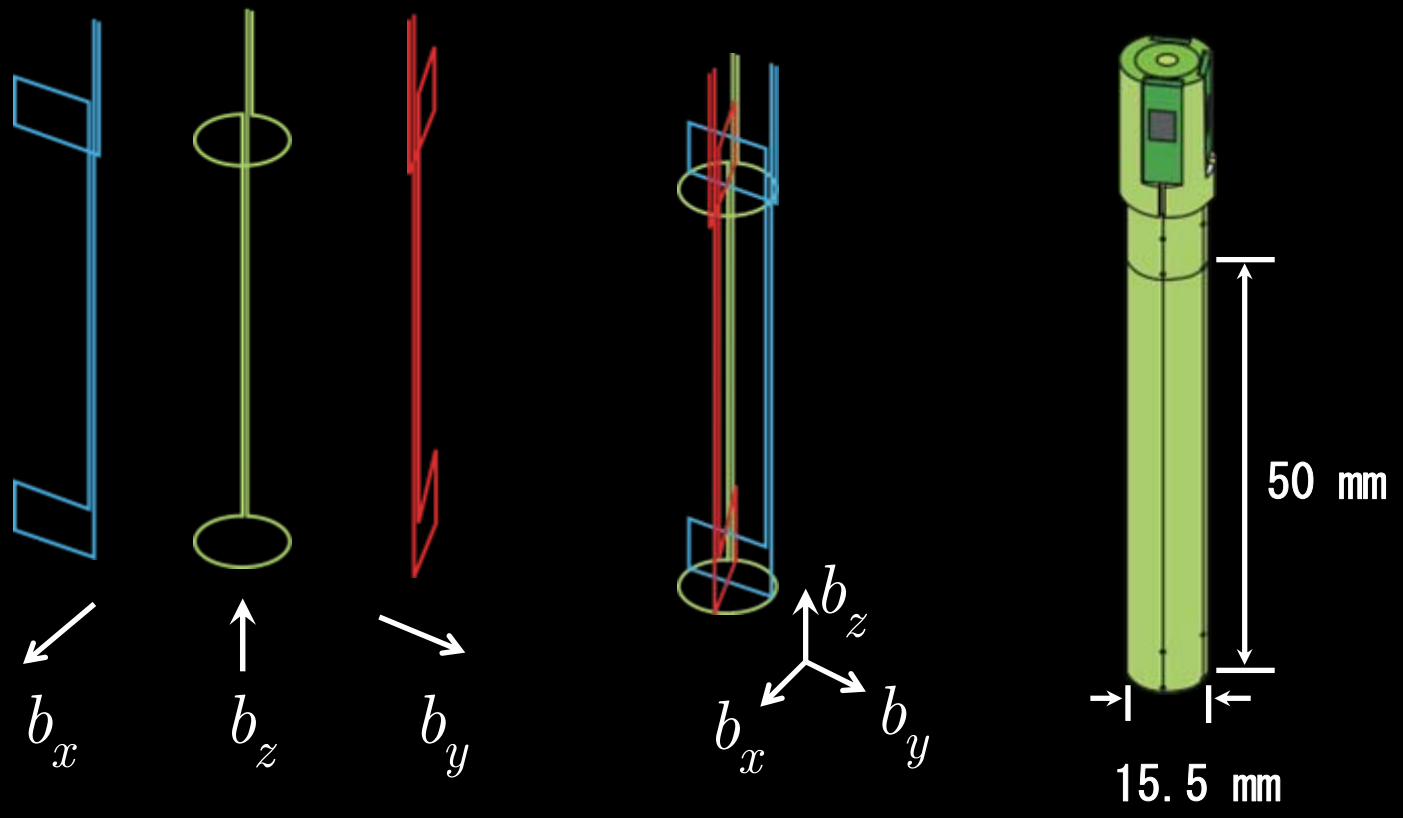


The sensor can detect three orthogonal components of the magnetic field $b_x$ , $b_y$ and $b_z$.

# Sensor array

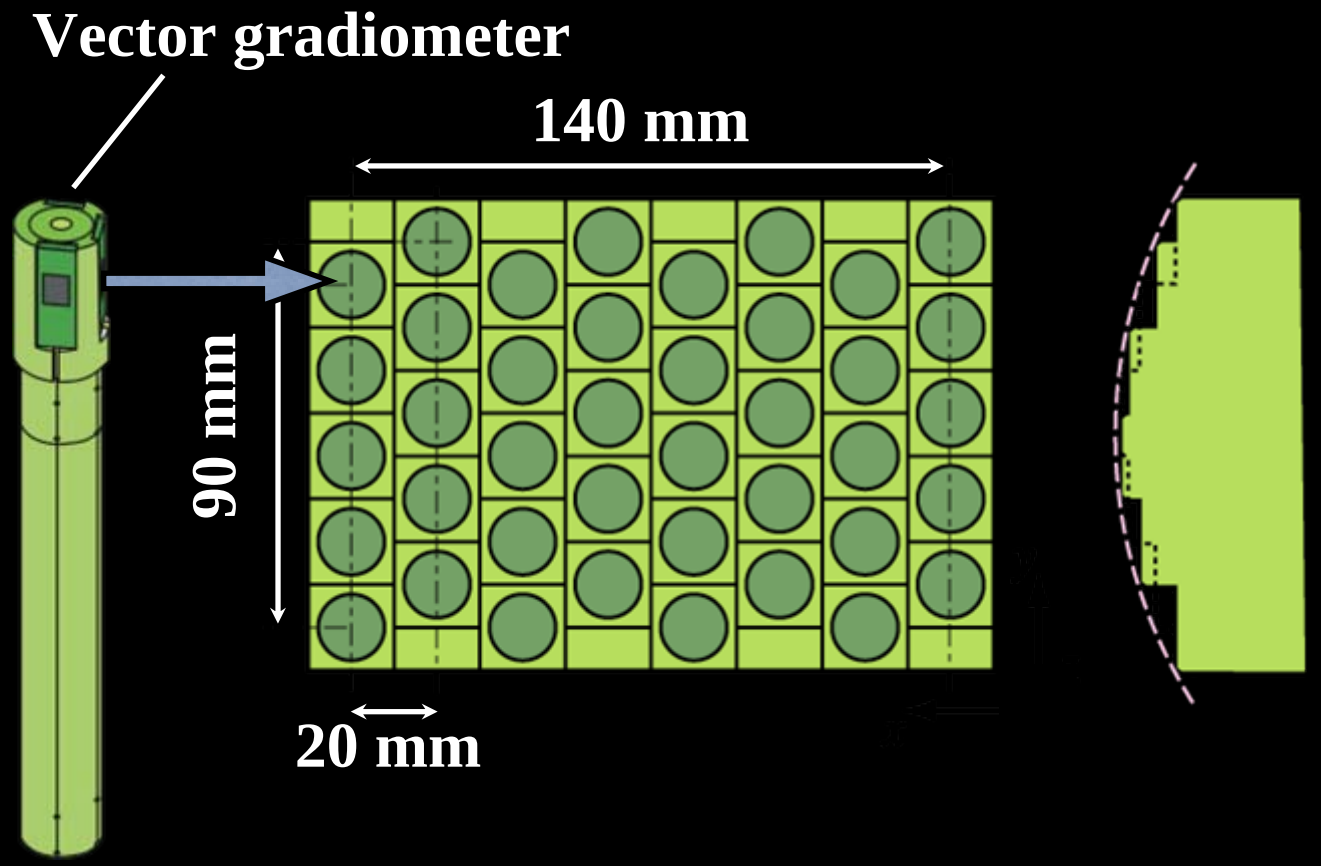



The array has 40 vector sensors consisting of a 5 by 8 matrix. The biomagnetometer has total 120 channels.

Sensors are aligned on a curved surface that is designed to fit to the subject's neck.

# Extraction of two dimensional plane containing spinal cord

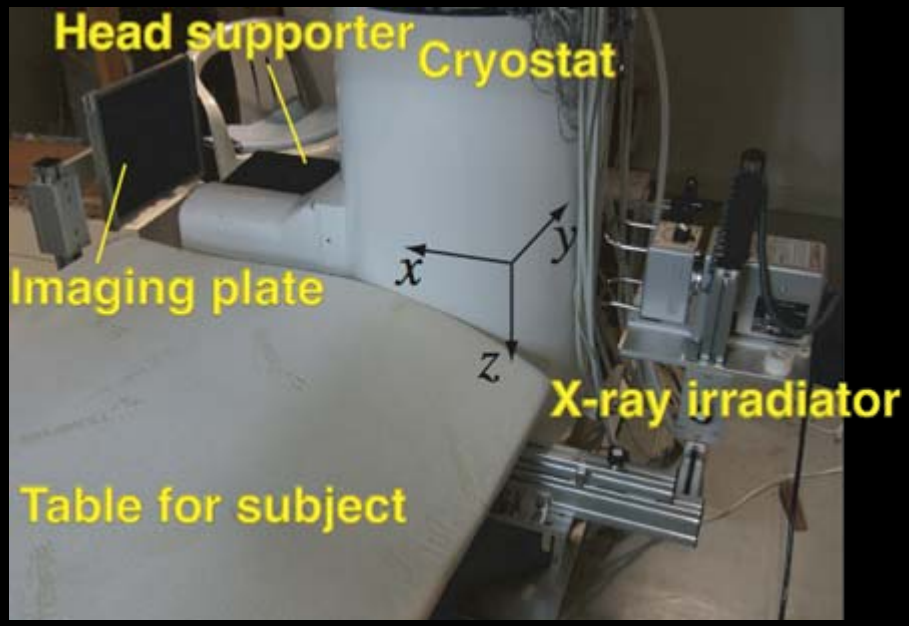


The biomagnetometer has an integrated X-ray imaging system.

An X-ray image of the subject neck and the sensors can be obtained for the positioning of the subject.

Extracted 2D source space

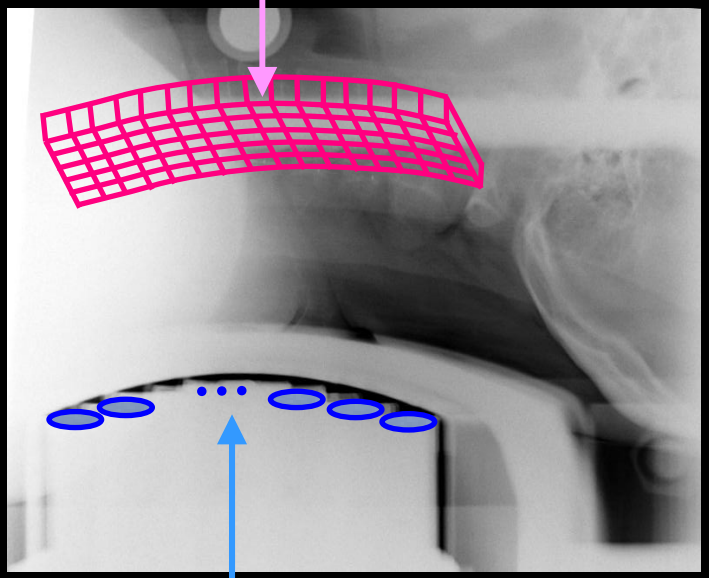

Sensor array

A plane containing the spinal cord is determined as the reconstruction region. the spinal cord source activity is reconstructed on this curved plane.

# Avoiding spurious change in source intensity

**Spurious intensity change is caused by non-uniformity of the distance between spinal cord and sensor array**

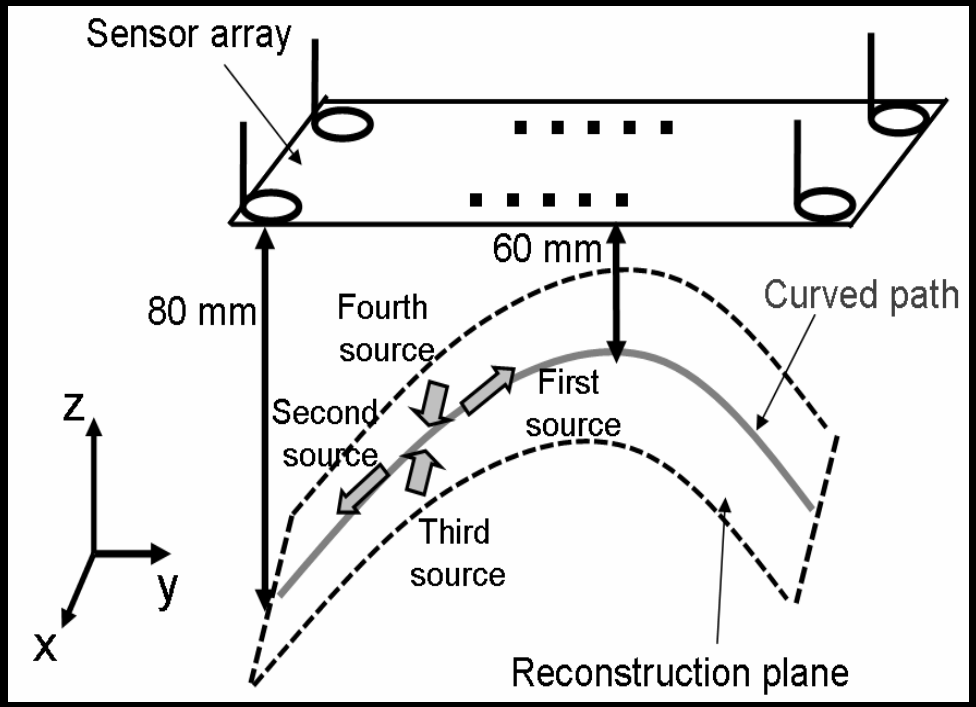


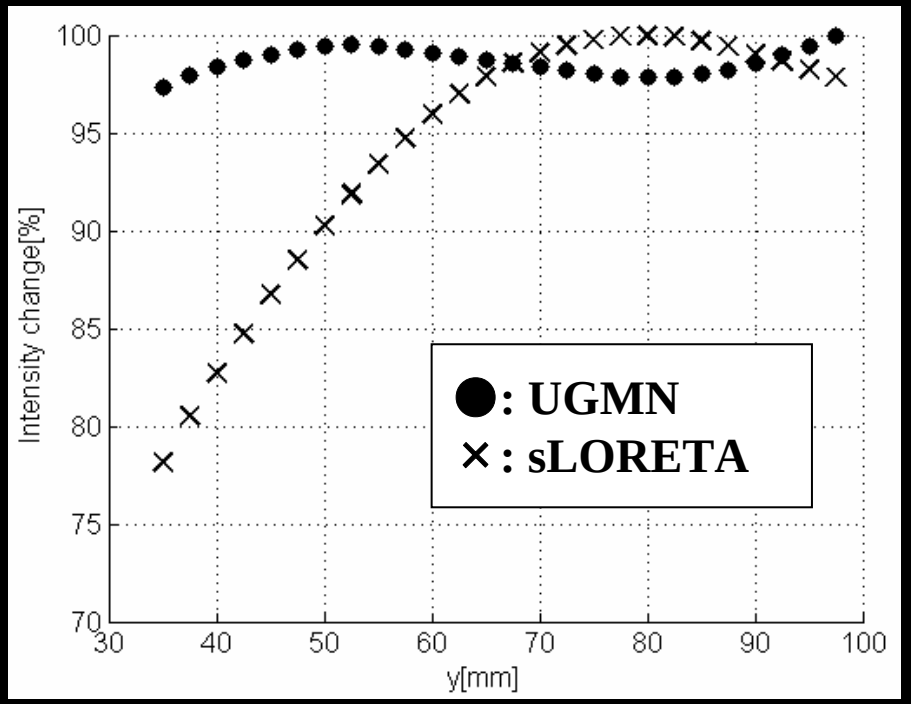


**Unit-gain constrained minimum-norm filter (Greenblatt, *et al* )**

$$\hat{s}(\boldsymbol{r},t) = \boldsymbol{w}^T(\boldsymbol{r})\boldsymbol{b}(t)$$

$$\boldsymbol{w}(\boldsymbol{r}) = \boldsymbol{G}^{-1}\boldsymbol{l}(\boldsymbol{r}) / \left[\boldsymbol{l}^T(\boldsymbol{r})\boldsymbol{G}^{-1}\boldsymbol{l}(\boldsymbol{r})\right]$$

# Data from a representative patient

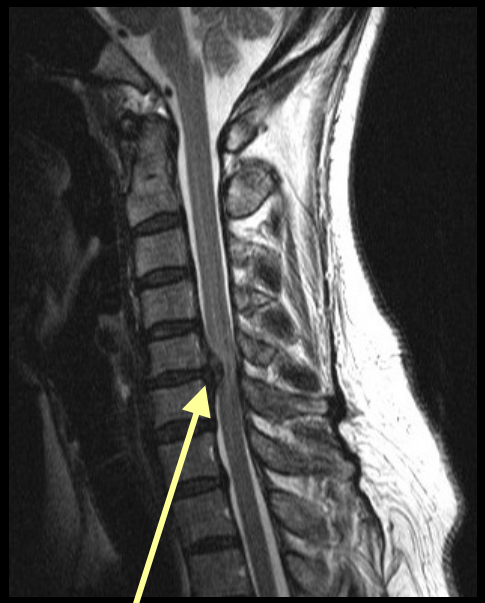

Patient: 47 years old, female

Stimulus condition:3mA, 0.3ms, 17Hz

Data acquisition: 40kHz sampling,
0.5-5kHz Bandpass filtering
4000 trials averaging

**Possible incomplete Conduction block between C5/C6.**

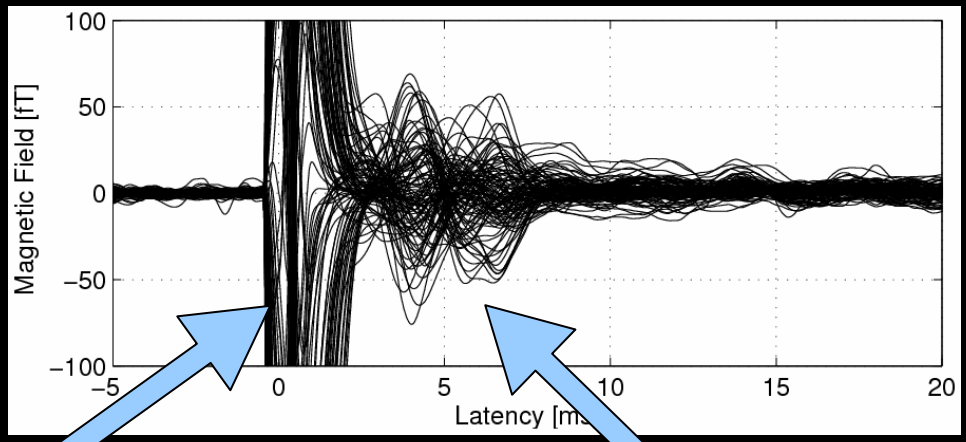


**Stimulus artifact**

**SCEF signal**

# Several snap shots of reconstructed spinal cord activity

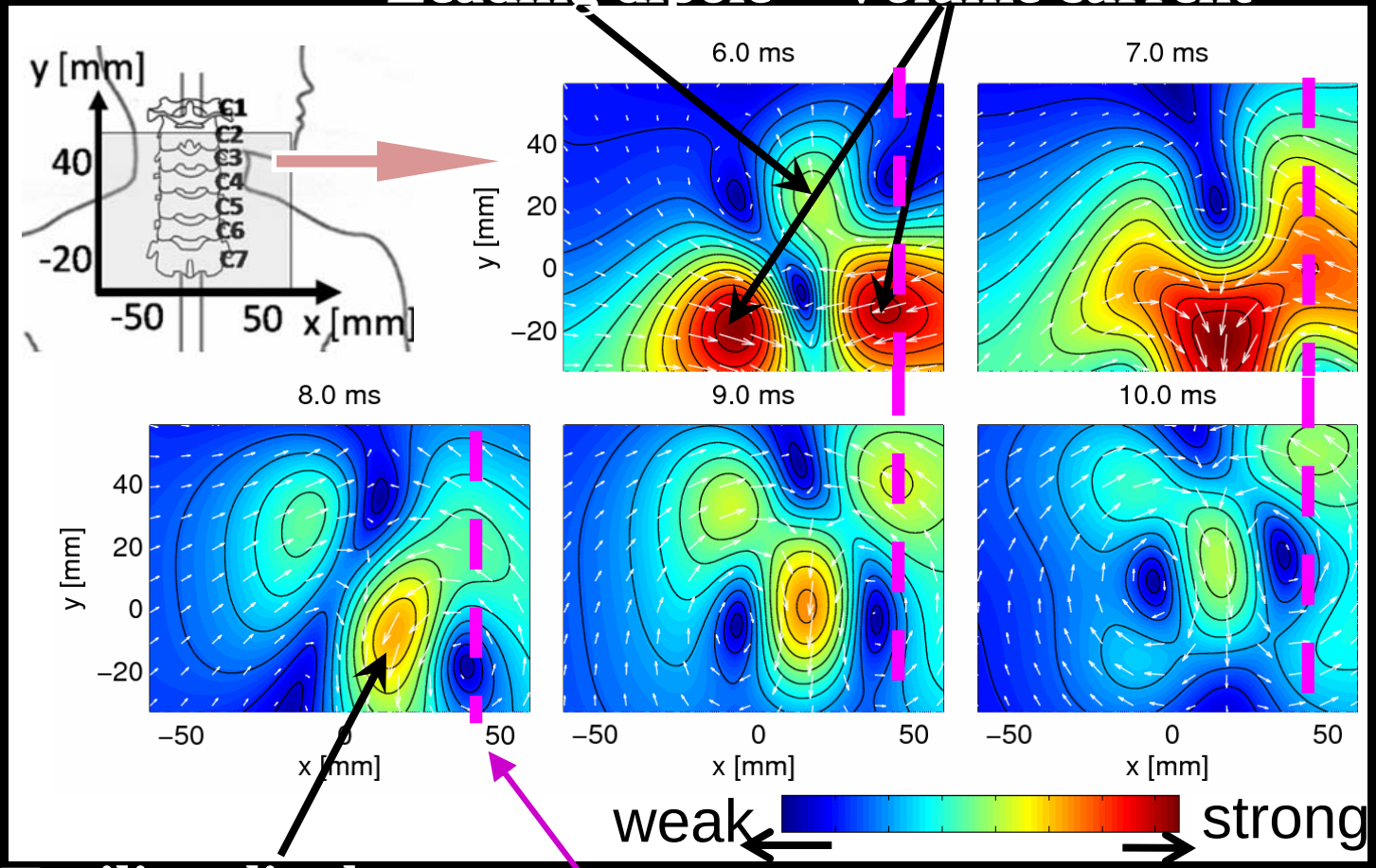

# Overlay of volume current intensity on patient's MRI

Voxels located on the volume current trajectory

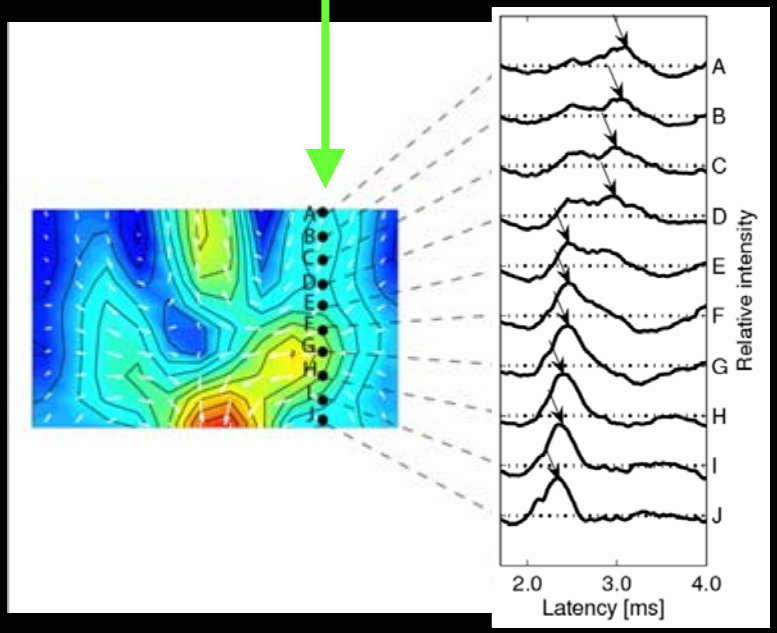


Conduction block is located between C5 and C6

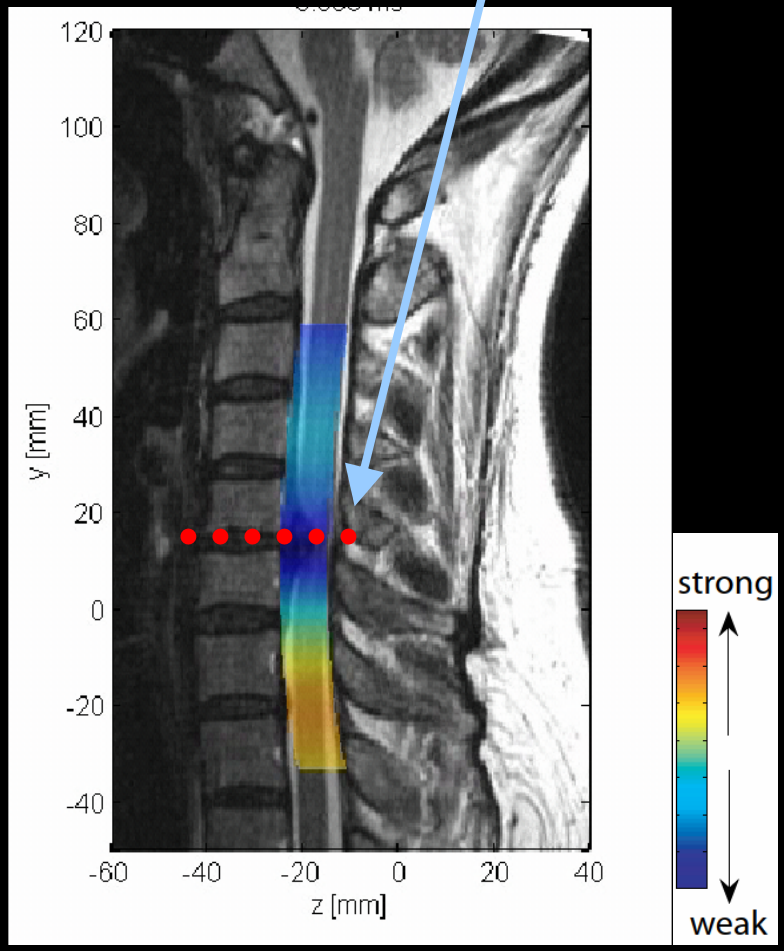


Intensity maximum over time is color-coded and overlayed on MRI

Intensity of the volume current decreases between C5 and C6

# Improved detection of volume current intensity change

## Voxel time course

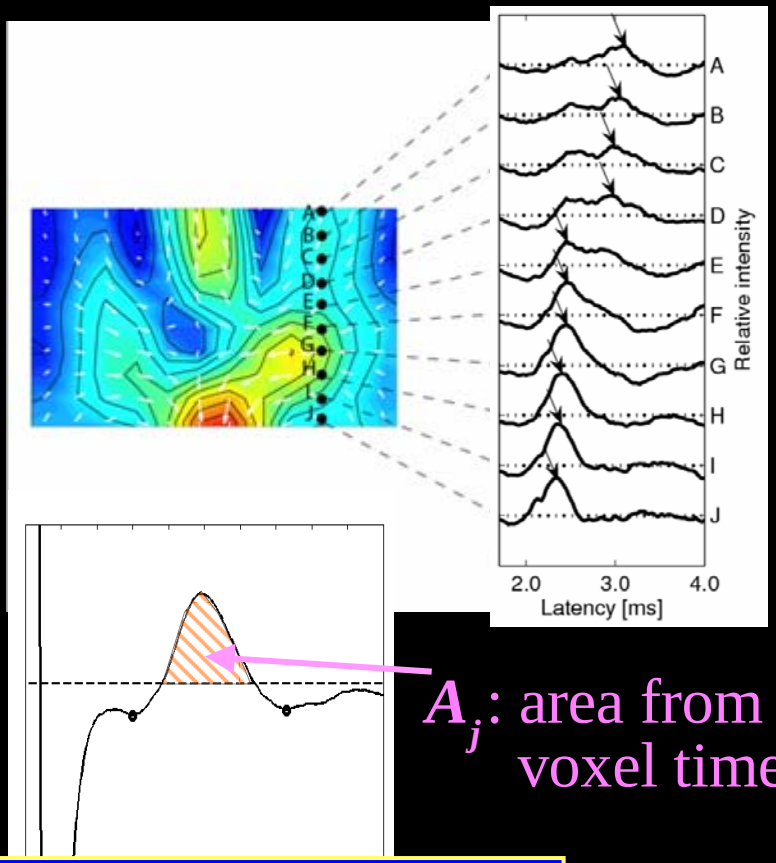


$A_j$: area from the $j$th voxel time course

Compute the area as the intensity measure

## Conduction block

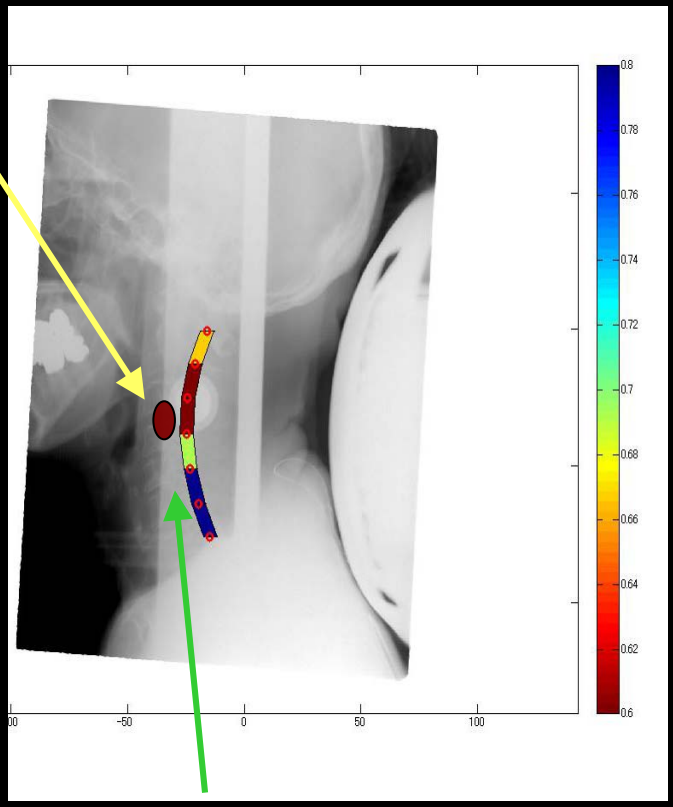

Color-coded plot of $A_j/A_{j-1}$ overlayed on subject X-ray image.

**So far, we have compared SCEF results with SCEP results for more than 40 patient cases, and have obtained 92% agreement.**

**A product sales promotion video made by Yokogawa Co.**

We are exploring the possibility for the detection of nerve conduction disorders in the lumber spine area using the same instrument

Possible nerve lesions detected in an anatomical MR image

**The number of patients with nerve disorders in the lumbar spine exceeds six hundred thousands in Japan**


Subject's lumbar region is positioned on the upper surface of the protrusion of the cryostat.

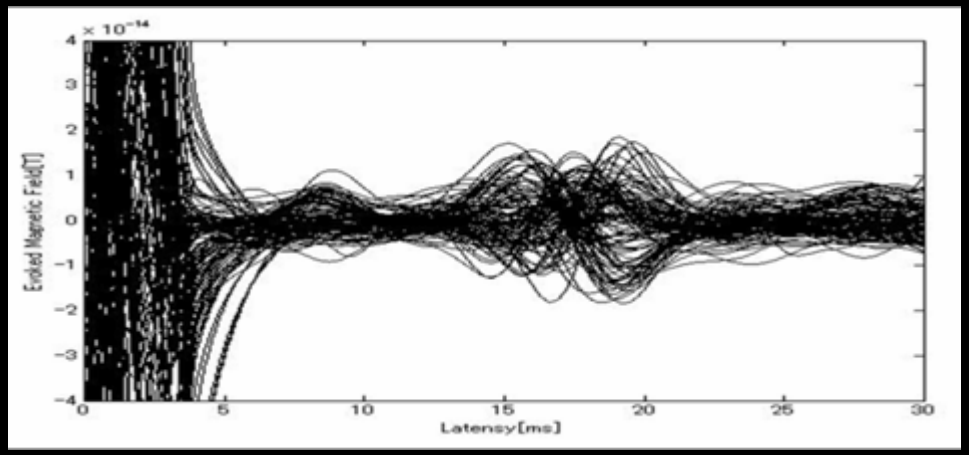


We can measure evoked magnetic field over the surface of lower back with stimulation on tibial nerve at ankle.

**Because the distance between the spine nerve and sensor array is larger in the lumber region, we need to use a spatial filter with higher spatial resolution.**

**Minimum-variance spatial filter is well-known for its high spatial resolution. However, it cannot be applied to this problem, because a good sample covariance matrix cannot be obtained, due to the rapid movements of sources.**

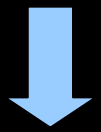

**We propose to use:**

# RENS (REcursively-obtained Null- Steering) spatial filter

**Kumihashi I, Sekihara K, "Array-gain constraint minimum-norm spatial filter with recursively updated gram matrix for biomagnetic source imaging" IEEE Trans Biomed Eng, 57, 2010, 1358-65.**

# RENS spatial filter (1)

## Similarity between min-norm and min-variance spatial filters

Minimum-norm filter with unit-gain constraint

$$\boldsymbol{w}(\boldsymbol{r}) = \frac{\bar{\boldsymbol{G}}^{-1}\boldsymbol{l}^T(\boldsymbol{r})}{\boldsymbol{l}^T(\boldsymbol{r})\bar{\boldsymbol{G}}^{-1}\boldsymbol{l}(\boldsymbol{r})}, \text{ where } \bar{\boldsymbol{G}} = \int p(\boldsymbol{r})\boldsymbol{l}(\boldsymbol{r})\boldsymbol{l}^T(\boldsymbol{r})d\boldsymbol{r}$$

Minimum-variance adaptive spatial filter

$$\boldsymbol{w}(\boldsymbol{r}) = \frac{\boldsymbol{R}^{-1}\ \boldsymbol{l}(\boldsymbol{r})}{\boldsymbol{l}^T(\boldsymbol{r})\boldsymbol{R}^{-1}\boldsymbol{l}(\boldsymbol{r})} \text{ where } \boldsymbol{R} = \int \left\langle s(\boldsymbol{r},t)^2 \right\rangle \boldsymbol{l}(\boldsymbol{r})\boldsymbol{l}^T(\boldsymbol{r})d\boldsymbol{r}$$

**measurement covariance matrix**

If we set $p(\boldsymbol{r})$ to be something similar to $\left\langle s(\boldsymbol{r},t)^2 \right\rangle$, the weighted minimum-norm filter should perform like the minimum-variance filter.

# RENS spatial filter (2)

**We use a recursive procedure.**

set $p(\boldsymbol{r}) = const$

compute $\bar{\boldsymbol{G}} = \int p(\boldsymbol{r})\boldsymbol{l}(\boldsymbol{r})\boldsymbol{l}^T(\boldsymbol{r})d\boldsymbol{r}$ and $\boldsymbol{w}(\boldsymbol{r}) = \dfrac{\bar{\boldsymbol{G}}^{-1}\boldsymbol{l}(\boldsymbol{r})}{\boldsymbol{l}^T(\boldsymbol{r})\bar{\boldsymbol{G}}^{-1}\boldsymbol{l}(\boldsymbol{r})}$

compute $\hat{s}(\boldsymbol{r},t) = \boldsymbol{w}^T(\boldsymbol{r})\boldsymbol{b}(t)$

set $p(\boldsymbol{r}) = \left\langle \hat{s}(\boldsymbol{r},t)^2 \right\rangle$ or $p(\boldsymbol{r}) = \hat{s}(\boldsymbol{r},t)^2$ for single-time-point data

RENS spatial filter has the spatial resolution much higher than those of min-norm-based spatial filters, and can be applied to single time-point data.

# Reconstructed results for comparing the min-norm filter and the RENS filter using actual signals from the lumber spine

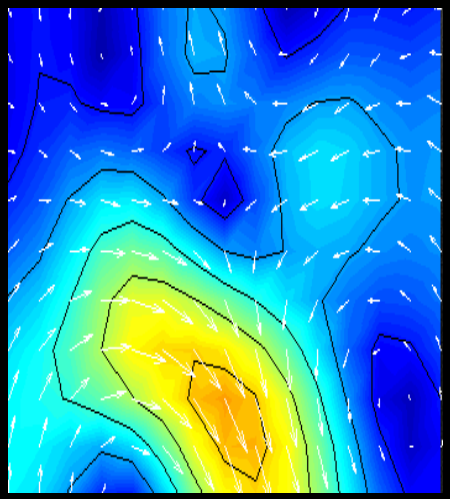

UGMN filter

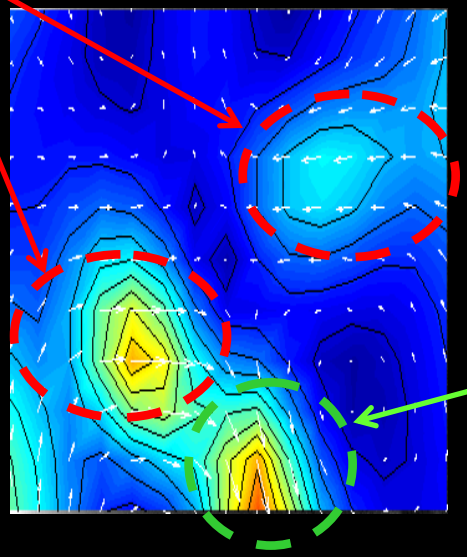


RENS filter

The RENS spatial filter can resolve volume current sources from dipoler sources; they are not resolved by Min Norm filter.

# Volume current trajectory cannot be approximated as a straight line in the lumber region.

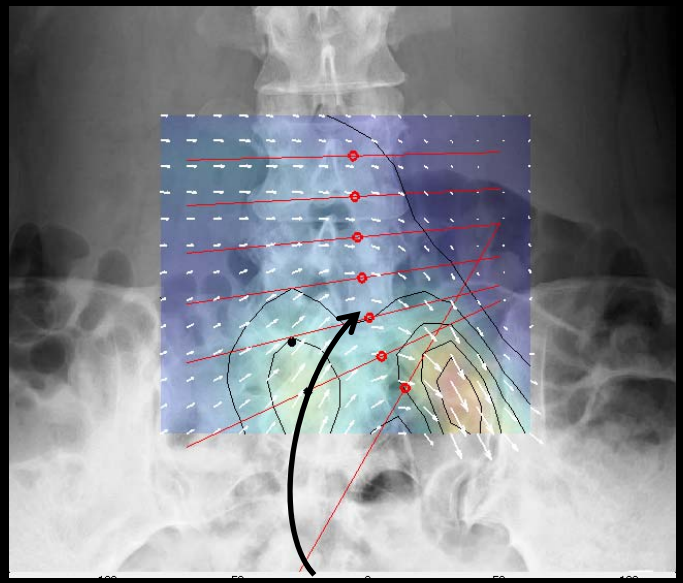

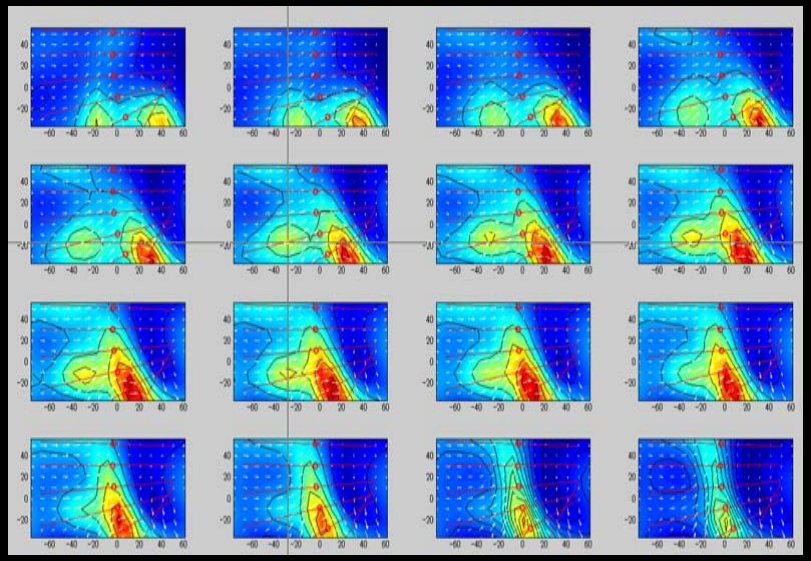

- Nerve location is estimated from the trajectory of leading dipole.

- Volume current intensity is estimated as the intensity in the direction normal to the nerve.

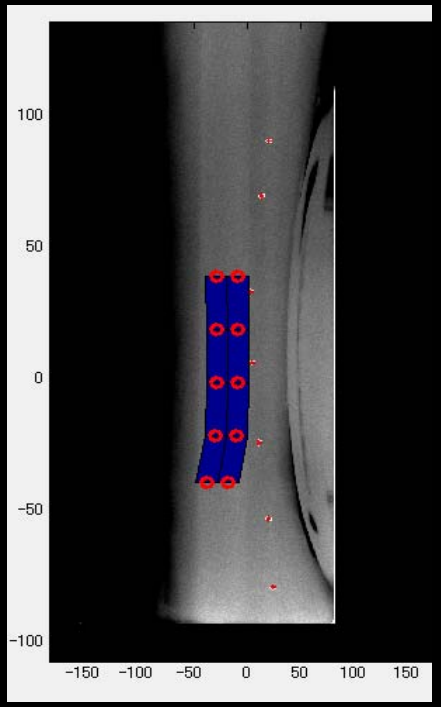


Healthy volunteer

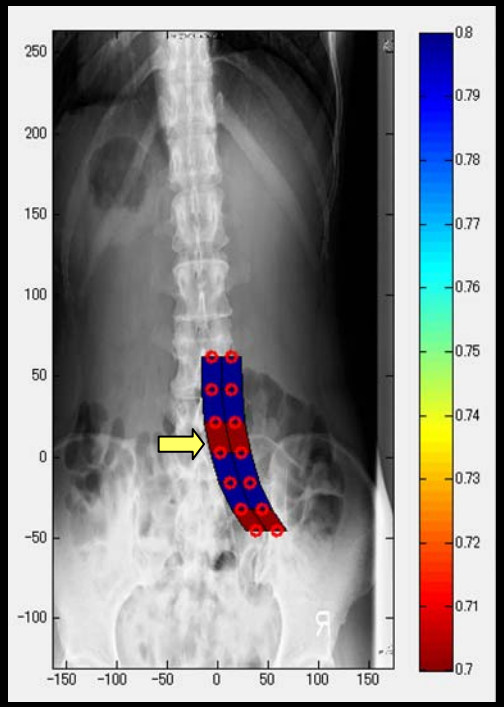


Patient with a conduction disorder

# Conclusions

**We have developed spinal cord functional imaging for clinical diagnosis of spinal cord conduction disorders.**

**Spinal cord imaging of patient's neck region:**

- **We have compared SCEF results with SCEP results for more than 40 patient cases, and we have obtained 92% agreements.**

**Spinal cord imaging of lumber spine:**

- **We are now exploring the possibilities, and have obtained promising results from several patients.**

Thank you very much for your attention